



ELSEVIER

Physica B 318 (2002) 387–391

PHYSICA B

www.elsevier.com/locate/physb

Organic–inorganic perovskites for magnetic nanocomposites

Etienne Wortham^a, Andrej Zorko^b, Denis Arcon^b, Alexandros Lappas^{a,*}^a *Institute of Electronic Structure & Laser, Foundation for Research & Technology – Hellas, P.O. Box 1527, 71110 Heraklion-Crete, Greece*^b *Institute “Jožef Stefan”, Jamova 39, 1000 Ljubljana, Slovenia*

Abstract

Two-dimensional perovskite compounds of the $(C_nH_{2n+1}NH_3)_2MnCl_4$ ($n = 2, 9$) type have been synthesised by a solid-state chemistry route in order to act as the building blocks for organic–inorganic magnetic nanocomposite materials. Depending on the amine chain length, the corresponding interlayer lattice expansion was probed by powder X-ray diffraction, and analysed by the *LeBail* method of profile matching. These perovskites undergo a transition to an antiferromagnetic state ($T_N = 40–43$ K). The low-dimensional magnetic behaviour characterised by both SQUID susceptibility and ESR measurements is marginally affected by the varying width of the organic layer separator. We discuss possible chemical routes for the incorporation of these lamellar alkyl amine perovskites in a polymer matrix to obtain new nanocomposite materials, which will support magnetic characteristics of the parent perovskite compounds. © 2002 Elsevier Science B.V. All rights reserved.

PACS: 75.75.+a; 81.20.–n; 61.10.–i; 76.30.–v

Keywords: Perovskites; Hybrid materials; Diffraction; Magnetism; Exfoliation

1. Introduction

Organic–inorganic hybrid materials can provide very useful properties by coupling together characteristics of organic (e.g. plasticity, efficient luminescence) and inorganic compounds (e.g. magnetism, electrical mobility) in the molecular level [1].

Hybrid perovskites can provide interesting magnetic nanocomposite materials. The layered perovskite $(C_nH_{2n+1}NH_3)_2MnCl_4$ family is known as a good example of quasi two-dimensional (2-D) Heisenberg antiferromagnet [2]. The structure consists of infinite $MnCl_4^{2-}$ sheets made up of corner-shared $MnCl_6$ octahedra alternating with

organic cation bilayers (in the case of protonated primary amines). There is a shift of each successive perovskite sheet resulting in a staggered configuration of the layers (Fig. 1a). The ammonium head (NH_3^+) of the alkylammonium occupies the holes formed by the corner-shared $MnCl_6$ octahedra [3,4]. The organic chains are rarely perpendicular to the perovskite sheets and a little interdigitation between the organic layers generally occurs. The latter two factors have a direct influence on the distance, d between the inorganic layers as the length of the alkylammonium chains increases.

In this paper, we report the synthesis of $(C_nH_{2n+1}NH_3)_2MnCl_4$ perovskites by a solid-state chemistry route with a purpose to exploit them for building blocks in organic–inorganic magnetic nanocomposite materials. Both ethylammonium

*Corresponding author. Fax: +30-810-391305.

E-mail address: lappas@iesl.forth.gr (A. Lappas).

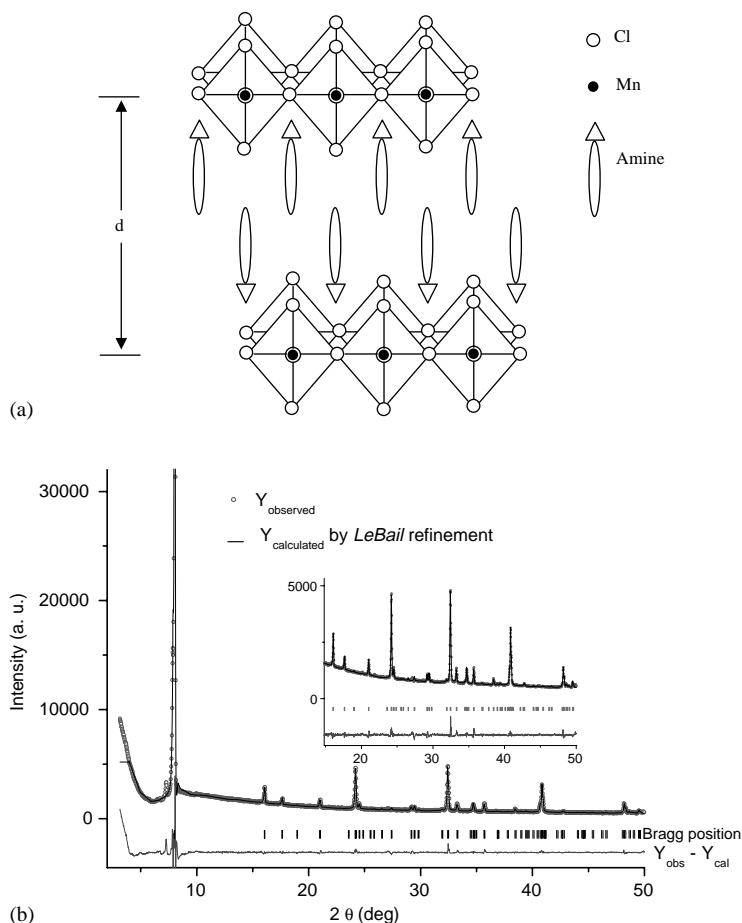


Fig. 1. (a) An illustration of the ideal lamellar crystal structure of $(C_nH_{2n+1}NH_3)_2MnCl_4$ perovskites. (b) XRD (Cu-K α radiation) powder pattern of $(EA)_2MnCl_4$ and its *LeBail* refinement. Observed (points), calculated (full curve) and difference (bottom curve) profiles are shown. Vertical tick-marks indicate Bragg reflection positions.

(EA: $n = 2$) and nonylammonium (NOA: $n = 9$) have been intercalated in the interlayer space. Magnetic susceptibility (SQUID) and CW X-band electron spin resonance (ESR) measurements were carried between 4.5 and 300 K to characterise the low-dimensional antiferromagnetic ground state of these materials. In order to disperse the perovskitic layers in an organic matrix some tests of exfoliation have been done as well.

2. Synthesis

In a controlled atmosphere (Ar) dry glove box, we mixed intimately high-purity $MnCl_2$ and

alkylammonium salt powders with the molar ratio 1:2. The mixture was sealed in a glass tube under argon atmosphere and then heated for five days at 150°C. The powder was ground and then heated for two additional days at 200°C for the ethylammonium $\{(EA)_2MnCl_4\}$ compound and at 230°C for the nonylammonium $\{(NOA)_2MnCl_4\}$ one.

3. Results and discussion

The lattice parameters of the $(EA)_2MnCl_4$ and the $(NOA)_2MnCl_4$ were followed by the *LeBail* method of profile matching through powder X-ray (Cu-K α radiation: on a Rigaku D/MAX-2000)

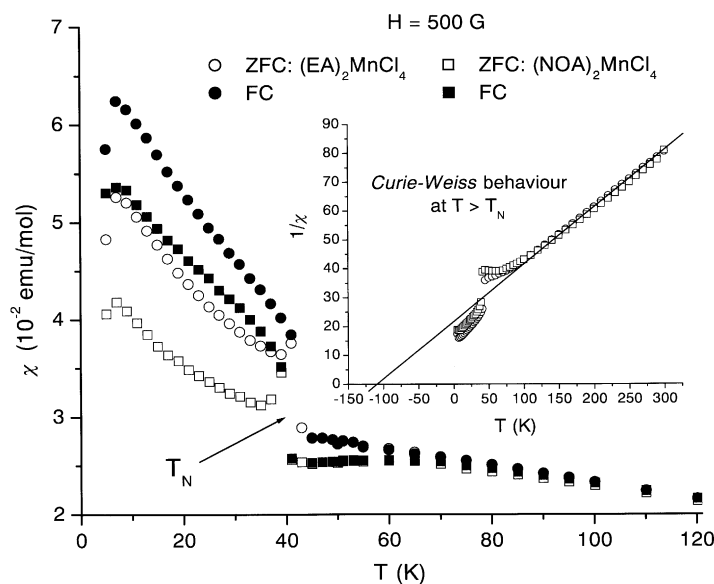


Fig. 2. Temperature dependence of the zero-field cooled (full symbols) and field-cooled (open symbols) DC magnetic susceptibility of $(\text{EA})_2\text{MnCl}_4$ and $(\text{NOA})_2\text{MnCl}_4$, measured in a magnetic field $H = 500$ G. Inset: inverse molar susceptibility ($1/\chi$) versus temperature. Straight lines indicate the Curie–Weiss fit at $T > T_N$.

Table 1
DC magnetic susceptibility results for $(\text{EA})_2\text{MnCl}_4$ and $(\text{NOA})_2\text{MnCl}_4$

	T_N (K)	θ (K)	μ_{eff} (μ_B)
$(\text{EA})_2\text{MnCl}_4$	43	-119(1)	2.04(3)
$(\text{NOA})_2\text{MnCl}_4$	40	-114(3)	2.02(1)

diffraction (Fig. 1b). The data confirmed the single phase of both compounds, and analysed satisfactorily in an orthorhombic unit cell (space group: Cmca), with lattice parameters: $a = 7.359(1) \text{ \AA}$, $b = 7.263(1) \text{ \AA}$, $c = 22.098(1) \text{ \AA}$ ($R_{\text{wp}} = 7.82\%$, $\chi^2 = 17.6$) and $a = 7.32(2) \text{ \AA}$, $b = 7.28(2) \text{ \AA}$, $c = 52.99(2) \text{ \AA}$ ($R_{\text{wp}} = 16.5\%$, $\chi^2 = 21.3$) for $(\text{EA})_2\text{MnCl}_4$ and $(\text{NOA})_2\text{MnCl}_4$, respectively, with no extra un-indexed Bragg reflections. We note that depending on the amine chain length, the corresponding interlayer spacing (i.e. c -axis direction) increases with the chain length, whereas the other parameters show little variations and do not depend significantly on the number of carbon atoms in the amine. These values are very close to those given in the literature for perovskites

synthesised by an aqueous solution route [5,6]. In comparison to this earlier work the present method of synthesis leads to well crystalline materials with similar pronounced 2-D character in their structure.

The DC magnetic susceptibility (χ) properties were measured for both compounds (Fig. 2). The materials undergo a phase transition from paramagnetic to antiferromagnetic phase at low temperatures in agreement with literature for analogous perovskite systems [6,7]. The magnetic data above the characteristic ordering temperatures (T_N) were analysed with a Curie–Weiss law and the fitted parameters are collected in Table 1. Importantly, and as reflected in the magnitude of the observed T_N 's the magnetic behaviour is marginally affected by the varying width of the organic layer separator. The robustness of the magnetic state upon substitution of the organic species supports a 2-D nature of magnetic interactions in our organic–inorganic perovskites, while the negative values of θ suggest the presence of antiferromagnetic correlations. The low experimental values of $\mu_{\text{eff}} \approx \sqrt{8\chi T}$ (Table 1), compared to the predicted Mn^{2+} free-ion value

($\mu_{\text{eff}} \sim 5.92\mu_B$; $S = \frac{5}{2}$) are worthy of further discussion. There may be various physical and chemical factors each one affecting the moment size to a different extent. For example, some temperature dependence in μ_{eff} , arising from changes of the thermal population between low- and high-spin states of Mn^{2+} , may account for deviations of the experimentally determined μ_{eff} from that in the free-ion. Also, the pronounced low-dimensional (2-D) character of the present perovskitic structures should give rise to ‘zero-point’ spin fluctuations [8] that would lead to a reduction in the magnitude of the localised Mn-moments. Moreover, the nucleophilic behaviour of the Cl^- ions can lead to strong covalency with the metal cations, in effect decreasing further the size of the μ_{eff} .

Magnetic properties of both samples were further studied by the ESR method. ESR intensity, which is proportional to the electron static susceptibility in the paramagnetic phase mimics the DC susceptibility measured by the SQUID. Below 40 K ($\sim T_N$), the ESR signal disappears almost completely due to the magnetic ordering. As we worked on powdered samples, we were not

able to detect antiferromagnetic resonance modes. More interesting is the temperature dependence of the ESR line width (Fig. 3). The temperature dependence of the ESR line width can be divided into two temperature regions: above the minimum around $T = 70$ K where the line width increases linearly with temperature (inset of Fig. 3) and the one below the minimum, but still above T_N , where the line width increases very sharply with decreasing temperature. We suggest that the temperature dependence of the ESR line width in the latter, fluctuation region is determined by the non-linear excitations or solitons [9]. A fit to the theoretical model yield the excitation energies $E_S = 673$ and 570 K for $(\text{EA})_2\text{MnCl}_4$ and $(\text{NOA})_2\text{MnCl}_4$, respectively (Fig. 3). These values are in an excellent agreement with the theoretically obtained excitation energy $E_S = 4\pi J_s^2$ [9]. Critical fluctuations due to the coupling to spin-waves are, however, dominant only very close to T_N .

Although experiments are still in progress, including these lamellar alkyl amine perovskites in a polymer matrix (e.g. PMMA; $M_W = 100,000$) by an exfoliation process indicate (e.g. optically clear, non-refractory film formation) that

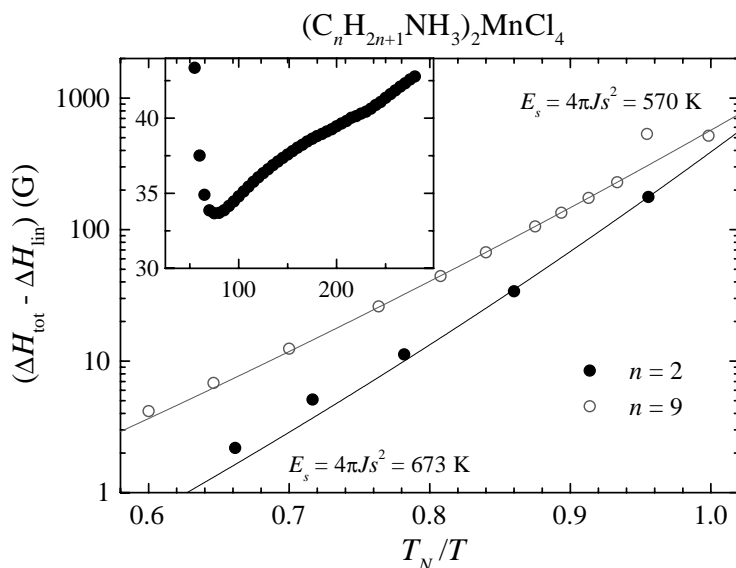


Fig. 3. The temperature dependence of the ESR line width in the vicinity of the magnetic transition (T_N) in $(\text{EA})_2\text{MnCl}_4$ and $(\text{NOA})_2\text{MnCl}_4$. The solid lines represent the fit to the soliton-driven temperature dependence of the ESR line width (see text for more details). Inset: the full temperature dependence of the ESR line width for $(\text{EA})_2\text{MnCl}_4$.

molecular entities composed of single alkyl amine MnCl_6 layers may maintain the characteristic properties (e.g. magnetism) of the parent 2-D perovskite compound. Earlier studies in this direction employing magnetic $\gamma\text{-Fe}_2\text{O}_3$ nanocrystals embedded in a polymer matrix by ion exchange method [10] inspired us in the search for new compounds exhibiting novel phenomena. It is suggested that the molecular like character of the perovskite building blocks (whose solubility in the organic matrix may be controlled by the varying length of the amine), would minimise the degree of their aggregation and could further couple to the intrinsic properties of the organic matrix material to lead to novel nanocomposite materials. Their characterisation is under way and will be reported elsewhere.

4. Conclusions

A solid-state chemistry route was employed in the synthesis of $(\text{C}_n\text{H}_{2n+1}\text{NH}_3)_2\text{MnCl}_4$ ($n = 2, 9$) perovskites. X-ray diffraction resolved the lamellar character of the structure, while SQUID and ESR measurements probed that their 2-D antiferromagnetism remained the same irrespective of the thickness of the intercalated organic layer. The robustness of the magnetic ground state supports the candidacy of the organic–inorganic perovskites for active magnetic nanocrystals embedded in a non-magnetic organic matrix. It is expected that the novel composite material thus formed main-

tains some of the characteristics of the parent compound due to the intrinsic low-dimensional properties of the latter.

Acknowledgements

The present work was supported by the European Union through a Marie Curie Fellowship (Contract no. HPMD-CT-2000-00050). We thank M.A. Green (Royal Institution of Great Britain) for help with the SQUID measurements.

References

- [1] D.B. Mitzi, In: K.D. Karling (Ed.), *Progress in Inorganic Chemistry*, Vol. 48, 1999.
- [2] W.D. van Amstel, L.J. de Jongh, *Solid State Commun.* 11 (1972) 1423.
- [3] D.B. Mitzi, *J. Chem. Soc., Dalton Trans.* 1–12 (2001).
- [4] G. Chapius, R. Kind, H. Arend, *Phys. Stat. Sol. A* 36 (1976) 285.
- [5] W. Depmeier, J. Felsche, G. Wildermuth, *J. Solid State Chem.* 21 (1977) 57.
- [6] S. Flandrois, N.B. Chanh, R. Duplessix, Th. Maris, P. Negrier, *Phys. Stat. Sol. A* 149 (1995) 697.
- [7] N. Achiwa, *Phase Transitions* 28 (1990) 79.
- [8] L.J. de Jongh, *Solid State Commun.* 65 (1988) 963.
- [9] C.E. Zaspel, J.E. Drumheller, *Int. J. Mod. Phys.* 10 (1996) 3649.
- [10] J.K. Vassiliou, V. Mehrotra, M.W. Russell, E.P. Giannelis, R.D. McMichael, R.D. Shull, R.F. Ziolo, *J. Appl. Phys.* 73 (1993) 5109.